Photonics **2015**, *2*, 719-744; doi:10.3390/photonics2020719

OPEN ACCESS

photonics

ISSN 2304−6732

www.mdpi.com/journal/photonics

Review

Unlocking Spectral Versatility from Broadly−Tunable Quantum−Dot Lasers

Stephanie E. White [†] **and Maria Ana Cataluna** [†,*]

School of Engineering, Physics and Mathematics, University of Dundee, Nethergate, Dundee DD1 4HN, UK; E−Mail: s.e.white@dundee.ac.uk

[†] These authors contributed equally to this work.

***** Author to whom correspondence should be addressed; E−Mail: m.a.cataluna@dundee.ac.uk; Tel.: +44−13−8238−6514.

Received: 21 May 2015 / Accepted: 16 June 2015 /Published: 22 June 2015

Abstract: Wavelength−tunable semiconductor quantum−dot lasers have achieved impressive performance in terms of high−power, broad tunability, low threshold current, as well as broadly tunable generation of ultrashort pulses. InAs/GaAs quantum−dot−based lasers in particular have demonstrated significant versatility and promise for a range of applications in many areas such as biological imaging, optical fiber communications, spectroscopy, THz radiation generation and frequency doubling into the visible region. In this review, we cover the progress made towards the development of broadly−tunable quantum−dot edge−emitting lasers, particularly in the spectral region between 1.0–1.3 μm. This review discusses the strategies developed towards achieving lower threshold current, extending the tunability range and scaling the output power, covering achievements in both continuous wave and mode−locked InAs/GaAs quantum−dot lasers. We also highlight a number of applications which have benefitted from these advances, as well as emerging new directions for further development of broadly−tunable quantum−dot lasers.

Keywords: lasers; tunable; quantum dots

1. Introduction

Since quantum dots (QDs) were realized in the 1970s and 1980s [1−3] and first implemented in lasers in the 1990s [4,5], they have proven to have many useful qualities, such as low threshold current

density [6], high output power [7] and wide wavelength tunability [8]. In the past years, a range of epitaxially−grown QD materials systems has emerged, able to cover the spectral region from 638 nm [9] up to 1.9 μm [10]. It is fair to say that, among the types of QD structures, InAs QDs based on GaAs substrates have been one of the most intensively investigated and developed materials systems, particularly in the 1–1.3 μm spectral region [11]. This review will focus on the achievements in the development of broadly−tunable edge−emitting QD lasers in this spectral region, based on InAs/GaAs materials. Such broadly−tunable lasers have a wide range of applications including spectroscopy [12], frequency doubling [13] and biomedical imaging modalities such as optical coherence tomography [14], as the wavelength range between 1–1.3 μm overlaps with regions of deep tissue penetration with minimal scattering. For this reason, QD lasers are also extremely promising laser sources for multiphoton microscopy, as recently demonstrated [15]. Moreover, their lower cost, complexity and footprint would also address the major shortcomings associated with the lasers currently used, which are bulky and high cost, as currently discussed in the bio−imaging community [16].

This review will first touch upon the distinctive features behind QD lasers and how these can be exploited in order to manipulate their spectral characteristics and enhance their tunability (for a much more in−depth coverage on the theory of QD lasers, please see [11]). A brief overview of the main architectures for implementing broadly−tunable lasers will follow. The state of the art will then be presented via the different strategies for improving the qualities of broadly−tunable QD lasers, including the reduction of threshold and operational current, the maximization of tunability range and output power, and the generation of tunable ultrashort pulses. All of these approaches are ultimately underpinned by the continual engineering of the semiconductor device structures themselves, as will be demonstrated. Finally, a number of applications benefitting from the use of tunable QD lasers will be explored, followed by an outlook for future developments of these promising systems.

2. Quantum−Dot Lasers: Exploiting Quantum Confinement and Inhomogeneous Broadening

At the core of QD lasers lies the concept of reduced dimensionality, as QDs are essentially semiconductor nano−sized clusters surrounded by a semiconductor matrix of higher bandgap. This is illustrated in Figure 1, where the density of states (N) for a bulk semiconductor is compared with that for semiconductors which display quantum−confinement in one, two and three dimensions, corresponding respectively to quantum wells, quantum wires and quantum dots. As the carriers are confined in all three dimensions in QDs, available states only exist at discrete energies, such as the ground state represented by the delta function in Figure 1. Due to this carrier confinement, QDs exhibit higher resilience to temperature effects. Theoretically QDs therefore have the similar basic properties of an atom, with clearly defined electronic transitions, but in reality can have a size distribution that leads to the broadening of their density of states.

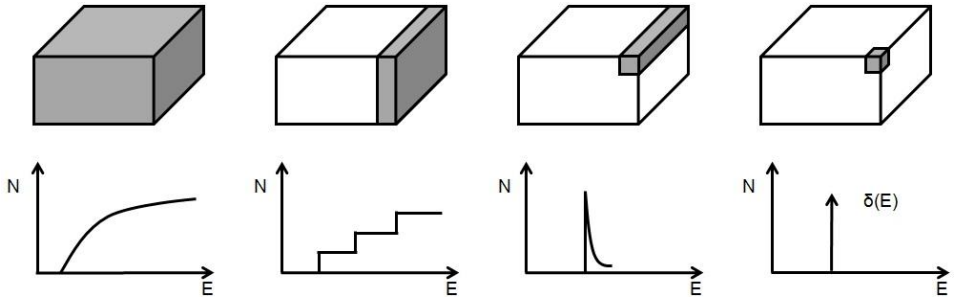

Figure 1. Geometry schematics and expressions for density of states (N) as a function of energy for: (from left to right) 3D bulk, 2D quantum−well, 1D quantum−wire and 0D quantum−dot semiconductor structures [17].

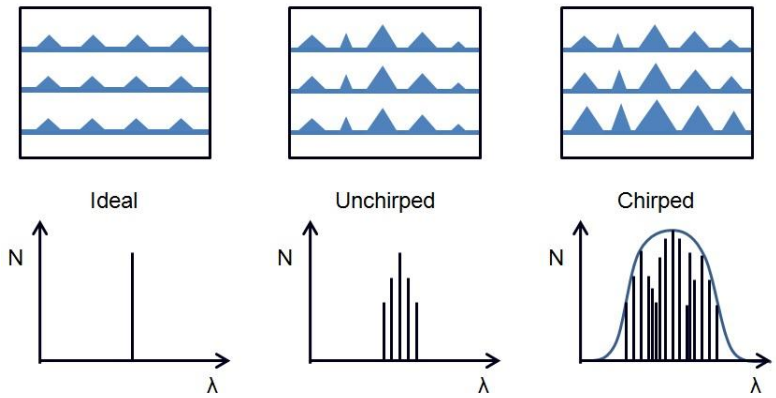

Figure 2. Schematic representation of ideal, unchirped (identical) and chirped (non−identical) quantum dot layers, with their corresponding density of states, considering only the ground state. With additional excited state transitions, it may be possible to tune continuously between the ground state (GS) and excited state (ES), thanks to the inhomogeneous broadening of typical QD structures.

Discussions about QDs and the possibility for their use as the active region of a laser were purely theoretical until their first growth in 1985 [3] and the first demonstration of laser emission via photopumping [4] and electrical injection in 1994 [5]. Different growth techniques were developed, based on molecular beam epitaxy (MBE) and metal organic chemical vapor deposition (MOCVD) to form a variety of different QD materials, for example quantum−dot−in−a−well, single and multi−layer structures [11]. Due to the nature of Stranski−Krastanov growth during QD formation, characterized by 2D wetting layer plus 3D island growth, a distribution of quantum dot sizes exists in each layer grown, leading to a small amount of intrinsic inhomogeneous broadening of the gain [11], as illustrated in Figure 2. The drive towards the development of QD lasers with lower threshold and higher temperature insensitivity has led to tremendous efforts to reduce such inhomogeneous broadening as much as possible, as it implicates a departure from the ideal QD scenario, and thus negates, to some extent, the advantages aforementioned. Indeed, it is well known that an increasing level of inhomogeneous broadening leads to an increase in transparency and threshold current and a reduction of the modal and differential gain [18,19]. However, such inhomogeneous broadening and the resulting wider gain bandwidth can also be harnessed to great advantage in a range of devices such as

mode−locked lasers [20], broadband superluminescent diodes and lasers [21], as well as broadly−tunable lasers [7,22].

In order to take advantage of such quantum confinement effects and inhomogeneous broadening, a number of growth techniques have been developed to engineer further broadening of the gain, not only within a QD layer, but also from layer to layer, creating non−identical or chirped layers (Figure 2). The most immediate way to increase the inhomogeneous broadening would be by increasing the size dispersion, as proposed in [23]. An approach was then to consider changing the amount of InAs deposition in the QDs; however, this led to high variations on areal density and radiative efficiency from layer to layer [24,25].

Typically, InAs QD layers are capped with InGaAs strain relaxation layers (also called capping layers), and then separated by GaAs barriers, which are then embedded in $Al_xGa_{1-x}As$ cladding layers.

Another possibility is to engineer these InGaAs capping layers, either changing their composition (indium concentration) [26−29] or their thickness [21]. The spectral shift in emission is attributed to a strong reduction in the InAs strain allowed by thicker InGaAs capping layers due to lattice constant mismatch between the QDs and their substrate [30]. Another factor contributing to the broad gain bandwidth is the spinodal decomposition of the capping layers, leading to indium segregation from the capping layers into the quantum dots [31]. The average size of the quantum dots in a particular plane is therefore proportional to the thickness of its capping layer, with a corresponding change in spectral emission. The main advantage of this technique as opposed to manipulation of the InAs QD deposition is that the QD areal density is not changed, in addition to allowing better control of the gain spectrum. Furthermore, by then exploiting not only the ground but also the excited states, the gain bandwidth can be broadened even further.

3. Broadly−Tunable Lasers: Typical Architectures

Most broadly−tunable laser diodes are placed within an external cavity laser (ECL) containing a reflective diffraction grating (a grating−coupled external cavity laser, or G−ECL), used as a wavelength dispersive element due to the repetitive groove structure embedded in the surface of the grating. The dispersion of light by the surface of a grating is governed by the grating equation:

$$\mathrm{d}(\sin\theta_m) = m\lambda \quad (1)$$

which states that incident light normal to a diffraction grating with groove spacing d will diffract light with a wavelength of λ at angles θ_m with respect to the grating normal, where $m = 0, 1, 2 \ldots$ is an integer referring to the order of diffraction [32]. This can be expanded to the grating equation for light of any incidence angle θ_i:

$$d(\sin\theta_m + \sin\theta_i) = m\lambda \quad (2)$$

In the Littrow configuration (shown schematically in Figure 3a), the gain element (which can be a laser diode, a semiconductor optical amplifier or a gain chip) typically has an antireflective (AR) coating on one side and is collimated onto a diffraction grating, where the first order diffraction is fed back into the diode. Here the angle of incidence and diffraction are the same, and $m > 0$, so Equation (2) for the Littrow configuration becomes

$$2d(\sin\theta_L) = m\lambda_L \quad (3)$$

with θ_L and λ_L being the Littrow angle and wavelength respectively. The main disadvantage of this setup is that as wavelength tunability is provided by rotation of the diffraction grating, the output then moves depending on the angle of rotation. Methods to fix the output position do exist, such as rotating through a suitable pivot or incorporating an additional mirror, but can be cumbersome to implement. This problem is also overcome in the Littman−Metcalf configuration (Figure 3b), whereby the diffraction grating is stationary but the reflection back into the diode is provided by an additional mirror, which can be rotated to provide wavelength tunability. Another solution is to use a quasi−Littrow configuration (Figure 3c), where the light is collimated onto the diffraction grating, and the diffracted light is then fed back through the diode, for spectrally selective laser emission.

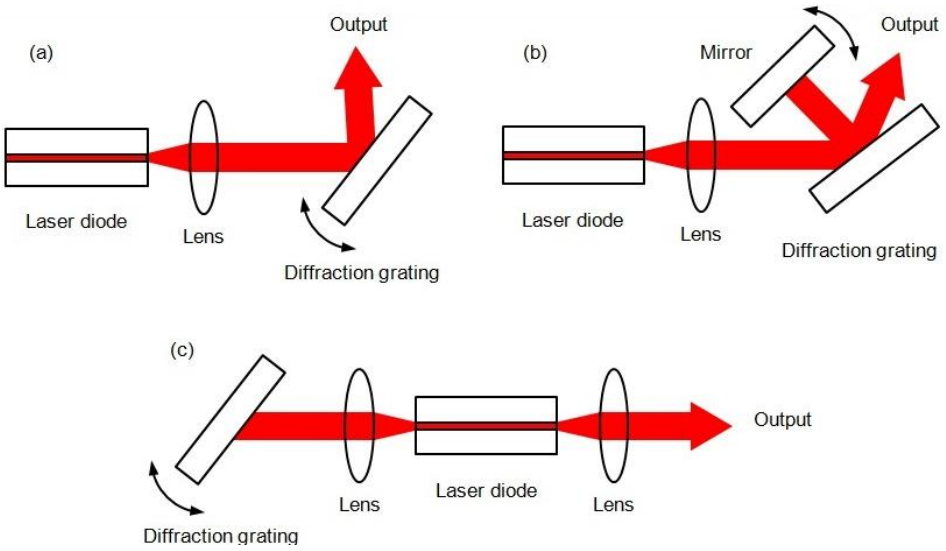

Figure 3. (**a**) Littrow; (**b**) Littman−Metcalf; (**c**) Quasi−Littrow configurations for wavelength tuning of a laser diode/gain chip.

Each of these schemes come with their own advantages: while the Littrow and quasi−Littrow setups are the easiest to implement and enable higher output powers [7] (and are thus the most popular), the Littman−Metcalf cavity is capable of achieving very narrow linewidths [33]. Other schemes might simply incorporate a tunable filter and/or a Fabry−Perot etalon in the cavity instead of a diffraction grating [34]. In monolithic QD tunable lasers, tunability has been demonstrated through the use of distributed Bragg reflector embedded in the laser [35], through the manipulation of the bias conditions in multi−section devices [36,37] and via optical injection techniques [38].

4. State of the Art in the Development of Continuous Wave Tunable QD Lasers

In order to improve the capabilities of tunable QD lasers, many performance goals have been targeted, such as threshold current density, power output, linewidth and tuning range. An up to date summary of tunable InAs/GaAs QD lasers operated in continuous wave (CW) can be found in Table 1, describing the laser setups and output characteristics. This is followed by a more detailed discussion of the various development strategies.

Table 1. Summary of tunable InAs/GaAs QD lasers operated in CW between 1.0–1.3 μm, with leading attributes in bold. [RWG: ridge waveguide; SOA: semiconductor optical amplifier; OC: output coupler; SNSS: sandwiched sub−nano separator growth technique].

Year	Laser Details	Minimum Threshold I_{th}/J_{th}	Maximum Power	Peak λ/Linewidth	λ Tuning Range	Ref.
2000	30 μm × 2 mm diode, 1x InAs QD layer in InGaAs QW, in a G−ECL (Littman−Metcalf)	88 mA 0.147 kA/cm^2	120 mW (peak power)	1231 nm	28 nm (1212–1240 nm)	[39]
2000	9 μm × 2 mm RWG, 1 × InAs QD layer in InGaAs QW, in a G−ECL	45 mA 0.25 kA/cm^2	10 mW (peak power)	1230 nm / < 3 nm	150 nm (1095–1245 nm)	[40]
2000	9 μm × 1.7 mm RWG, 1 × InAs QD layer in InGaAs QW, in a G−ECL	0.3 kA/cm^2		1050 nm	201 nm (1033–1234 nm)	[41]
	9 μm × 2 mm RWG, 1 × InAs QD layer in InGaAs QW, in a G−ECL	0.25 kA/cm^2		1090 nm	183 nm (1070–1253 nm)	
2003	5 μm × 1.6 mm RWG, 7 × InAs/GaAs QD layers, in a G−ECL (Littrow)	235 mA 2.94 kA/cm^2		~1090 nm/ 0.8 nm	83 nm (1047–1130 nm)	[42]
2007	5 μm × 750 μm RWG laser diode (two separate sections 250 μm and 500 μm long), 5 InAs/GasAs QD layers. λ tuning by current change.	0.15 kA/cm^2		1023 nm / < 125 pm	11.7 nm (1017.4–1029.1 nm)	[37,43]
2007	100 μm × 1.5 mm diode in a Littman G−ECL	170 mA **0.113 kA/cm^2**	140 mW	1240 nm/ 0.07–0.1 nm	20 nm (1235–1255 nm)	[33]
2008	5 μm wide bent RWG, 10 non−identical InAs QD layers in a G−ECL		630 mW	1180 nm/ **200 kHz (0.9 fm)**	155 nm (1125–1280 nm)	[44]
2010	120 μm × 1 mm device, 5 layers of InAs QDs in a G−ECL	~0.57 kA/cm^2	65 mW	1120 nm/ < 2 nm	100 nm (1073.9–1173.8 nm)	[6]
	120 μm × 2 mm device, 5 layers of InAs QDs in a G−ECL	~0.22 kA/cm^2	53 mW	1180 nm/ < 2 nm	110.1 nm (1141.6–1251.7 nm)	
	120 μm × 3 mm device, 5 layers of InAs QDs in a G−ECL	0.117 kA/cm^2	54 mW	1240 nm/ < 2 nm	55 nm (1198.2–1253.1 nm)	

Table 1. *Cont.*

Year	Laser Details	Minimum Threshold I_{th}/J_{th}	Maximum Power	Peak λ/Linewidth	λ Tuning Range	Ref.
2010	5 μm × 4 mm gain chip based on 10 non−identical InAs QD layers in a G−ECL with 20% [or no] OC	2.0 kA/cm^2 [0.34 kA/cm^2]	138mW [480mW]	1150 nm [1220 nm]	197.5 nm (1127−1324.5 nm) [184.5 nm (1129–1313.5 nm)]	[22]
2010	5μm × 4mm SOA, 10 non−identical InAs QD layers in a G−ECL with 4% R OC	not stated	230 mW	1213 nm/ 0.12 nm	150 nm (1140–1290 nm)	[13]
2010	5 μm × 2.5 mm RWG, 11 non−identical InAs QD layers in a G−ECL	~2.15 A	200 mW	1200 nm/ ~1 nm	**207.7 nm (1038.3–1246 nm)**	[8]
2011	5 μm × 4 mm SOA, 10 non−identical InAs QD layers in a G−ECL	not stated	16 mW	1220 nm	120 nm sweep range (~1160–1280 nm)	[14]
2011	3.4 μm × 1.95 mm gain chip, 7 identical layers SSNS−grown InAs/InGaAs structure. ECL with narrow optical band−pass and etalon filters used for λ control.	60 mA 0.9 kA/cm^2	3.01 mW	1300 nm/ 210 kHz	56 nm (1265–1321 nm)	[34]
2012	5 μm × 1.5 mm RWG, 10 non−identical InAs QD layers in a G−ECL	100 mA 1.33 kA/cm^2	27 mW	1180 nm/ <0.5 nm	150 nm (1143–1293 nm)	[45]
	5 μm × 2 mm RWG, 10 non−identical InAs QD layers in a G−ECL	75 mA 0.75 kA/cm^2	37 mW	1240 nm/ <0.5 nm	130 nm (1160–1290 nm)	
	5 μm × 3 mm RWG, 10 non−identical InAs QD layers in a G−ECL	50 mA 0.33 kA/cm^2	40 mW	1260 nm/ <0.5 nm	63 nm (1218–1281 nm)	
2013	5 μm × 1.5 mm device, 10 non−identical QD layers in a double Littman G−ECL	50 mA 0.66 kA/cm^2	5.5 mW	1180 nm	Dual−wavelength tunability within 1150–1276 nm, with max λ separation of 126 nm	[46]
2014	6 mm long tapered SOA, width 14 μm at start, 81 μm at end, 10 chirped InAs QD layers in a G−ECL	500 mA 0.31 kA/cm^2	620 mW	1230 nm/ ~0.3 nm	96.8 nm (1195.8–1292.6 nm)	[7]
	6 mm long tapered SOA, width 14 μm at start, 81 μm at end, 15 identical InAs QD layers in a G−ECL	300 mA 0.24 kA/cm^2	**970 mW**	1254 nm/ ~0.3 nm	31.6 nm (1240.4–1272 nm)	

4.1. Optimization of Threshold Current

An important aspect of any laser design is the reduction in threshold current density (J_{th}), as this has effects on thermal management and overall laser efficiency. Since the very early development of tunable QD lasers, it was realized that a low threshold current density and wide tunability was possible owing to the effect of the low density of states for QDs causing easy saturation of the ground state optical gain–as the threshold is low, then higher energy levels may be populated by carriers at lower current densities in comparison with quantum−well (QW) lasers [39−41]. Indeed, to the best of our knowledge, the broadest tuning range achieved in a QW laser in this spectral region was enabled by an InGaAsP/InP multi−QW laser [47], resulting in a broad tuning range of 160 nm, centred at 1336 nm. However this laser achieved a maximum power of only 40 mW and this tunability range was only made possible for a current density of at least 64 kA/cm^2, which is at least over an order of magnitude higher than that associated with QD lasers for even broader tunability ranges. In fact, all of these characteristics (power, tunability, operation current) have been improved upon by QD lasers (as previously shown in Table 1). The apparent absence of subsequent work on equivalent broadly tunable QW edge−emitting lasers in the spectral region of 1.0–1.3 μm could possibly provide an indication that QD structures are now regarded as the first choice of materials for such developments.

Threshold current and tuning range are intrinsically connected and depend on whether the GS or the ES are accessed, and whether the QD structure contains chirped or unchirped layers. In this context, it is particularly useful to go back to those studies where a comparative investigation was made of several different structures or laser layouts. The first demonstration of a broadly tunable QD laser (201 nm) already provided key insights into the role of chip length and cavity loss in the achievable tunability [41]. Considering laser diodes with the same AR coatings, reducing their cavity length from 2 mm to 1.7 mm led to an increase in the free−running loss, enabling access to the more energetic excited states. As long as such an increase in loss does not exceed the saturated gain of the ground state, then it is possible to access both GS and ES and thus extend tunability [41]. This was further demonstrated in [6], whereby the tunability of an external cavity laser was investigated with diode chips of different lengths (1, 2 and 3 mm). It was observed that the laser containing the longest chip could only be tunable across GS transition, while the shortest chip only allowed for laser emission across the first and second excited states, requiring a threshold current over 8 times higher than that for the GS−emitting laser cavity containing the 3−mm chip [6]. As the gain threshold is also inversely proportional to the combined reflectivity of the cavity mirrors [32], it was also shown that a low reflectivity coating applied to the facets of the 3mm device reported in [6], also contributed to an 88% increase in the external cavity's J_{th}, but did however increase the tuning range from 55 nm to 145 nm, as it prevented solitary laser emission at higher pumping currents, allowing for an extended tunability range. This effect was also present in [42], where the threshold current of the solitary laser diode was increased by 100 mA by AR coating the output facet, enabling the external cavity laser to be operated at a pump current right below the (now higher) solitary laser diode threshold. Further papers have reported high threshold currents (I_{th}), but due to the large waveguide area of their QD devices these translate to low J_{th} in comparison to their smaller narrow ridge counterparts. In fact, the smallest J_{th} so far for a tunable QD laser was for [33], which despite having a moderately high I_{th} of 170 mA, actually had a very low J_{th} of 0.113 kA/cm^2. Another low threshold current density of 0.24 kA/cm^2 was reported in [35] and also in [7],

despite both having thresholds of ~300 mA. These two devices were both tapered structures, having a narrow straight waveguide on one side, with a flared section ending in a much wider facet on the output side [7,35]. Tapered waveguides offer the benefit of high power previously only seen in broad area diodes, while keeping the nearly diffraction−limited beam quality of narrow ridge waveguides [48]. Due to their large areas, these lasers are also more thermally efficient, i.e. the larger area has a higher capability of transferring away heat generated from pumping the chip at the high currents needed to generate high output power—these factors (high current/large area) combine to give low current densities.

4.2. Maximising Tuning Range

One of the fundamental aspects of any semiconductor laser design is the diode itself: the composition and dimensions of the active region of the laser. To maximise the tuning capabilities of a QD laser there must be a large broadening of the gain bandwidth and as discussed in section 2, there is a considerable amount of intrinsic inhomogeneous broadening due to the uneven growth of QDs. This can be hugely increased by using multiple layers of QDs and deliberately varying the thickness of their capping layers (see Figure 2), thus creating a wide range of QD sizes and wavelengths for the diode to lase if a tuning element is implemented. Many systems have utilised this structure of QD layers and have produced very broad tuning ranges of up to 208 nm and extended as far as 1.32 μm [8,22].

Most tunable QD lasers so far based on these varying thickness ("chirped") layer structures have managed to achieve tuning ranges of at least 100 nm (see Figure 4 for a direct comparison throughout the years of tunable QD laser development), which reveals a trend away from the use of unchirped towards a more general adoption of chirped QD layers. A record high tuning range of 208 nm was achieved in [8] at multiple currents for a chirped QD layer structure with a bent RWG to prevent solitary lasing of the diode at high injection currents. However, with this high potential for wavelength tunability stemming from inhomogeneous broadening comes a trade−off with a higher threshold and stronger temperature dependence of the threshold current [18]. With higher levels of inhomogeneous broadening in QD structures, their properties start to depart from those of an ideal QD material, to some extent negating the beneficial effects of reduced dimensionality. The modal and differential gain are therefore reduced, increasing the threshold and transparency currents. The temperature dependence of the threshold current is a result of the large distribution of states gained from the high amount of inhomogeneous broadening and so a larger amount of reservoirs are available for thermal filling [18]. These observations were also realized in our work [7], which was the first one to report on the investigation of a comparison between chirped and unchirped structures in the context of QD external−cavity tunable lasers [7].

As the tunability range increases with pump current (as further and further states are populated), it is very important that a very high operational current can be applied, without inducing the laser into solitary emission. As explained in the previous section, this has led to broader tuning ranges via the application of AR coatings. A step change in tunability and output power is achieved with the incorporation of a gain chip including a bent waveguide, such that the effective resulting reflectivity on the corresponding facet can be as low as 10^{-5}, thus increasing the solitary laser threshold significantly. This has led to the demonstration of broadband tunabilities in excess of 150 nm along with maximum

output power well over 200 mW [8,22,44]. Moreover, a comparison has also been made between the use of output couplers with low (4%) or high reflectivity (80%) in a broadly tunable G−ECL QD laser [22]. While the output power was lower for the higher reflectivity, the lower cavity loss enabled an extension of the tunability range towards the longer wavelengths corresponding to the GS transitions by as much as 11 nm [22].

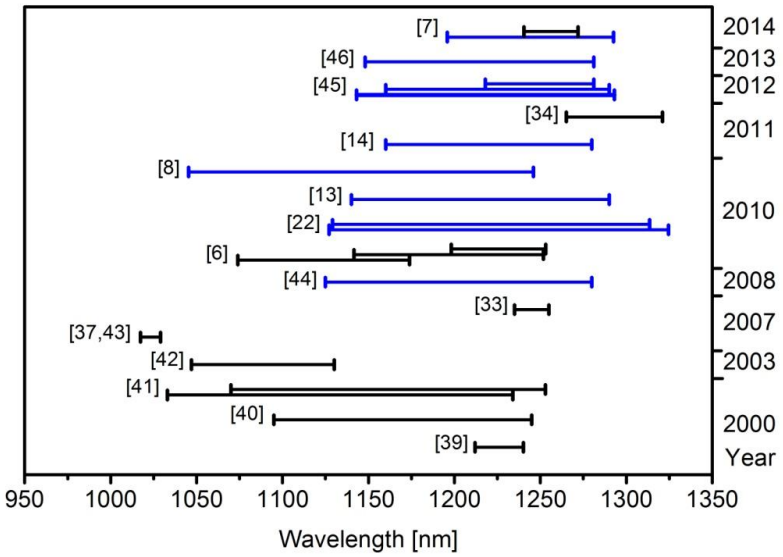

Figure 4. Progress of the tunability ranges along the years, for CW−emitting tunable InAs/GaAs QD lasers in the spectral range between 1.0–1.3 μm. QD lasers with chirped layer structures are shown in blue and even layers in black.

4.3. Maximising Power

Many tunable QD lasers, despite having a sizable tuning range, have a low output power, often only up to tens of mW [6,40,45]. While this may be acceptable for some applications (for example some methods of biological imaging where keeping the sample alive and undamaged is the priority [16]), other applications such as second harmonic generation can require a much higher output power. Driving the QD diode at higher currents also has the benefit of leading to significant broadening of the tuning range. In general, the limits associated with simply increasing the driving current are usually associated with solitary laser emission (as explained in the previous section) and/or thermal rollover.

Increasing the applied current to a diode can however lead to problematic overheating of the device. To this end many systems employ a pulsed current bias, enabling a high peak power while the average current delivered to the diode is low. For example, the optical spectrum's bandwidth of the laser in [21] was expanded to 75 nm by increasing the applied current and so the output peak power was pushed as far as 0.8 W. The largest tuning range so far from a quasi−CW pumped device however has been from [8], where nearly 208 nm of tunability was obtained with a maximum output power of 200 mW.

In any case, purely CW lasers have also succeeded in achieving high power and high tunability performance. Broad tunability of 155 nm and 202 nm from similar gain chips incorporating QD diode chirped structures were achieved in [44] and [22] with high maximum output powers of 630 mW and 480 mW, respectively. Recently, we have presented a setup with a new approach to power scaling,

which is currently the highest power achieved by a tunable QD ECL so far in its wavelength range [7]. Two SOAs were investigated in the same quasi−Littrow setup (Figure 5), with a cavity designed for maximum power and tuning range. As current was delivered in two separate sections, this allowed for a finer optimization of the output power. The SOAs both had tapered waveguides and AR coatings on each facet. The difference was in their QD layer structure: the first SOA had a chirped layer structure with three QD layers designed for output at 1211 nm, three at 1243 nm and four at 1285 nm. In contrast, the second SOA contained 15 layers of QDs all designed to emit at 1254 nm. As shown in Figure 6, the merits of these were compared, and the cavity containing the unchirped SOA only achieved 32 nm of tunability but a record output power of 0.97 W. The chirped SOA was found to have a much larger tuning range of nearly 100 nm and a maximum power or 0.62 W but a higher threshold current than the unchirped SOA, which is associated with the performance trade−offs between gain and inhomogeneous gain broadening in QD structures [7]. These high powers represented 12.5 and 19.6−fold increases in power for the chirped and unchirped SOAs respectively in comparison to the highest power previously achieved by a tunable QD laser in the same wavelength range, for the same current density [7,22].

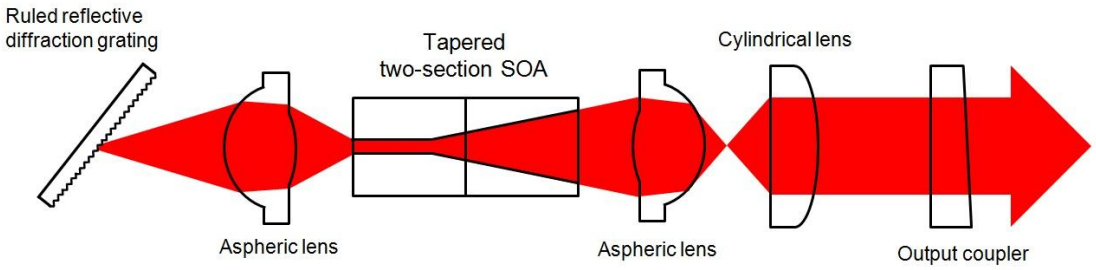

Figure 5. Plan−view schematic for the quasi−Littrow design used in [7]. A "cat's eye" cavity design is used between the SOA and the diffraction grating for enhanced stability and insensitivity to misalignment. Light from the front facet is collimated in the fast axis and astigmatism in the slow axis is corrected for by the cylindrical lens. About 4% reflectivity is provided back into the cavity by the output coupler. The SOA is tilted by 7°, but that is not represented here for simplicity (schematic not to scale).

At this point, it is opportune to compare the performance achieved thus far with optically−pumped QD VECSELs (Vertical External−Cavity Surface−Emitting Lasers), which by virtue of their external cavity, also enable the implementation of mechanisms for broad tunability. Beyond 1200 nm, the widest tunability range demonstrated from a QD VECSEL was 60 nm, which exploited the epitaxial variation across the wafer (typical of MBE), to enable tunability between 1220–1280 nm as the pump beam's position was changed in the gain mirror, with output power up to 400 mW [49]. Another demonstration of tunable QD VECSELs in the 1–1.3 μm spectral region made use of a birefringent filter to tune the wavelength within the cavity, where three different QD materials were tested, each incorporating a set of identical QD layers [50]. For the 1040 nm sample, a maximum wavelength tunability of 60 nm was achieved, while for the 1180 nm and 1260 nm samples, maximum tunabilities of 63 nm and 25 nm were demonstrated, respectively [50]. Such results were achieved with maximum output powers at the center of the tuning ranges of 2.2 W (1040 nm), 80 mW (1180 nm) and 550 mW

(1250 nm). Similarly to the case of edge−emitting external−cavity lasers, the choice of the output coupler's reflectivity dictated a trade−off between tunability range and output power—this was quite evident particularly in the 1180 nm sample, where a change from a 0.4% output coupler to a high reflector led to an expansion in tuning range from 23 nm to 69 nm, at the expense of a drop in maximum output power from 270 mW to 80 mW. As such, the record output power for a broadly tunable semiconductor laser in the 1.2–1.3 μm spectral region continues to hold for an edge−emitting QD laser as reported in [7], with a 32 nm tunability and a maximum output power of 0.97 W at 1254 nm. This comparison shows the significant promise in terms of wall−plug efficiency and simplicity associated with tapered−based external cavity QD lasers, operating at room temperature and using only thermoelectric cooling [7], considering that equivalent QD VECSELs are optically pumped and the highest power demonstrated required a diamond heatspreader and water cooling, down to a temperature of 5 ℃ [50].

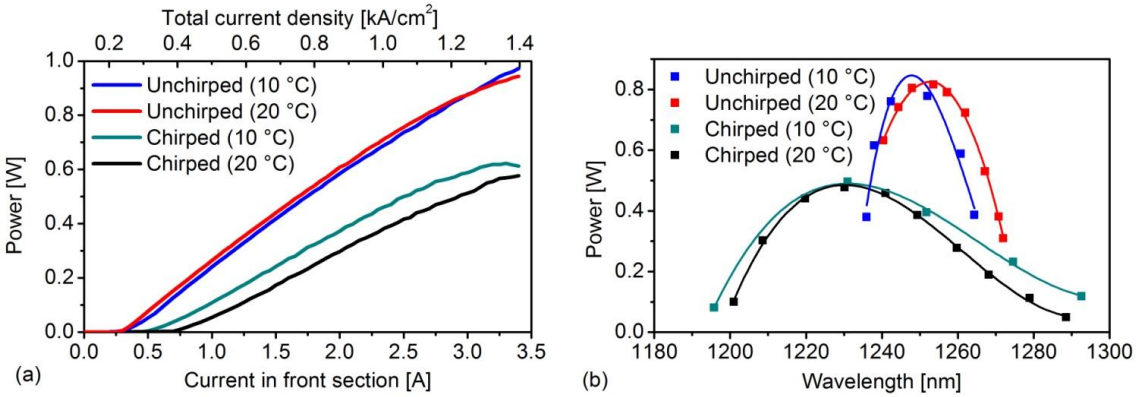

Figure 6. (**a**) Light−current and (**b**) tuning range characteristics of the chirped and unchirped lasers taken at different temperatures with I_R = 0.34 A in the smaller, straight rear section and a fixed value of I_F = 2.7 A in the much larger flared front section for the tuning ranges (Figures from [7]).

5. State of the Art in the Development of Tunable Mode−Locked QD Lasers

In addition to their spectral versatility, QD lasers have demonstrated a number of key advantages for the generation of ultrashort pulses [20,51,52]. The access to a broadband gain is not only relevant for access to a broad tunability, but also for supporting the generation of ultrashort pulses via mode−locking (ML). The exploitation of these features has resulted in a wide range of tunable mode−locked lasers, which are summarized in Table 2. As will be explored in this section, in addition to the variety of cavity layouts for enabling tunability, a range of mode−locking techniques can also be considered, leading to a substantial diversity of approaches that harness the broad bandwidth of both saturable gain and absorption associated with QD structures.

Indeed, the spectral versatility of QD lasers has also been shown to extend to both GS and ES, while ultrafast gain and absorption recovery have been demonstrated in both states as well [53,54]. The possibility of mode−locked operation engaging either of these states was demonstrated for the first time in a QD monolithic mode−locked laser, whereby the access to each state was controlled merely with the bias conditions [55,56]. Shortly after this demonstration, the possibility to tune the wavelength

around the central emission wavelength corresponding to these states was successfully exploited [57]. To this end, a quasi−Littrow grating−coupled external−cavity was built, incorporating a two−section gain chip based on 10 identical QD layers. A passive mode−locking regime was initiated via suitable forward and reverse bias applied to the gain and saturable absorber sections, respectively. Through the rotation of the diffraction grating, the first tunable QD ML laser enabled the generation of tunable ultrashort pulses across the GS (1265–1295 nm) and the ES (1170–1220 nm) [57]. A similar laser architecture was subsequently implemented, while using two−section gain chips with non−identical or chirped layers, which enabled for the first time the generation of ultrashort pulses continuously tunable from 1187 nm to 1283 nm [58]. By including a tapered SOA based on a chirped QD structure, the resulting master−oscillator power amplifier enabled a boost in the peak power to 4.39 W [58]. Subsequent optimization of the tunable oscillator led to the demonstration of short pulses with a 136 nm tunability, between 1182.5 nm and 1319 nm [59]. An alternative method to implement a passively mode−locked semiconductor laser relies on the use of a semiconductor saturable absorber mirror (SESAM), instead of a waveguide saturable absorber section. Using a QD gain device, this approach has been first demonstrated by using a QD SESAM as well [60], albeit at a fixed wavelength. Recent preliminary results have demonstrated a SESAM−based external−cavity QD passively mode−locked laser, whereby the central wavelength could be tuned by rotation of an intracavity prism, resulting in a tunability of 35.7 nm [61]. These recent results also report the lowest pulse repetition rate (f_{rep} = 520 MHz) demonstrated to date from a wavelength−tunable mode−locked QD laser (the overall lowest pulse repetition rate of 79.3 MHz has been demonstrated in [62], but no spectral tunability was demonstrated, and as such, it is not included in Table 2). Due to the flexibility with which the pulse repetition rate can be tuned, as previously demonstrated in passively−mode−locked QD lasers [62,63], there is significant scope for a range of QD tunable pulsed sources with repetition rates tailored to match particular applications of interest.

On the other hand, an active mode−locking approach has been pursued by Yamamoto and co−workers [64,65], whereby a single section device's current is modulated by an RF generator, at the same frequency corresponding to the inverse of its external−cavity roundtrip time. With the inclusion of an optical bandpass filter for wavelength tunability, the authors have demonstrated short pulse generation with tunability of 32 nm and 100 nm, respectively [64,65], using a chirped layer structure at the core of the device. While the latest reports do not present results on the noise performance of these lasers, it is anticipated that due to the presence of such active modulation, timing jitter resulting from active mode−locking can be substantially reduced in comparison with a passive mode−locking approach [66], whereas external cavity lasers also display lower timing jitter when compared to their monolithic counterparts [67]. All such features would certainly be of significance for the optical communications applications targeted by such developments.

An elegant alternative technique was demonstrated by Habruseva *et al.* [38], whereby a two−section mode−locked monolithic laser with a pulse repetition rate of 10 GHz was subject to optical injection of a master tunable laser with narrow linewidth (100 kHz). The master laser's output was modulated at a frequency which was half the pulse repetition rate of the slave laser, resulting in the generation of two coherent sidebands, separated by 10 GHz. While the main (and achieved) objective was the stabilization of the slave laser and reduction of its timing jitter, it was also observed that by tuning the master laser's wavelength, the slave laser's output could also be tuned by as much as 8 nm. Moreover,

this optical injection scheme resulted in a drastic narrowing of the optical spectrum of the slave laser (10 to 15−fold), while the pulse duration remained the same, leading to an associated reduction in time−bandwidth product and close to Fourier limit, with pulse durations down to 4.76 ps. Essentially, this constituted an alternative form of hybrid mode−locking, while also allowing for the tunability of the slave laser.

Other monolithic mode−locked QD lasers have also shown significant promise, by enabling the generation of ultrashort pulses at high repetition rates, whereby the wavelength could be tuned simply by varying the bias conditions applied to the gain and/or the saturable absorber sections. For instance, a dual−wavelength mode−locked quantum−dot laser was demonstrated with a spectral separation between the bands which was tunable with injection current within the GS band, varying between 2–14 nm [68], in a two−section laser with 5 identical QD layers. More recently, a continuous 45 nm tunability was reported from a mode−locked two−section monolithic laser with chirped QD layers [36], made possible by tuning the reverse bias applied to the saturable absorber. Owing to the absence of mechanical components, such results are of high interest as, for example, for swept laser systems, where the wavelength could be tuned at very high speeds. Considering that it is possible to have dual−wavelength mode−locking engaging both GS and ES simultaneously directly from a monolithic mode−locked QD laser [69], the results here presented are encouraging for the future development of broadly−tunable multi−wavelength mode−locked operation from QD lasers.

Table 2. Progress summary of mode−locked tunable QD lasers, with leading attributes in bold.

Year	Laser Details	Peak λ/ Spectral Bandwidth	λ Tuning Range	Maximum Power	Pulse Details	Ref.
2006	5 μm × 2 mm two−section device, 10 identical layers of InAs/GaAs QDs, G−ECL + 1.8 mm QD SOA	GS ~ 1274 nm ES ~ 1190 nm/ ~0.4 nm	GS: 30 nm (1265–1295 nm) ES: 50.5 nm (1170–1220 nm)	not stated	Passive ML. GS (λ = 1273 nm): Δτ = 6.6 ps. ES (λ = 1200 nm): Δτ = 12 ps. f_{rep} = 2.5 GHz.	[57]
2010	10 GHz devices, with a saturable absorber−to−total−length ratio of either 17% or 12%	1291–1299 nm	8 nm (1290–1298 nm)	1 mW average power	Passive ML + injection locking	[38]
2011	6 μm × 4 mm multi−section RWG, 5 layers of InAs/InGaAs QDs	1280 nm	λ separation of two GS sub−bands tunable by 2–14 nm		Passive ML, Δτ ~ 17ps, f_{rep} = 10 GHz.	[68]
2012	6 μm × 4 mm RWG gain chip in a G−ECL with 6 mm long tapered SOA, width 14μm at start, 81μm at end, both with 10 chirped InAs/GaAs QD layers	1226 nm/ ~2.5 nm	96 nm (1187–1283 nm)	**4.39 W** peak power (~92 mW average power)	Passive ML, shortest Δτ = 15 ps with 1.316 GHz f_{rep} achieved within λ tuning range conditions	[58]

Table 2. *Cont.*

Year	Laser Details	Peak λ/ Spectral Bandwidth	λ Tuning Range	Maximum Power	Pulse Details	Ref.
2012	6μm × 4mm RWG, 10 chirped InAs QD layers in a G−ECL	1226 nm/ ~1 nm	**136 nm** (1182.5–1319 nm)	870 mW peak power (10.5 mW average power)	Passive ML, Δτ = 12.8–39 ps, f_{rep} = 740 MHz.	[59]
2012	3.4 μm × 3.9 mm RWG, 7 non−identical InAs QD layers in an ECL. λ tuning by band−pass filter	1294.9 nm/ 0.25 nm	32 nm (1262.9–1294.9 nm)		Active ML, Δτ = 10–15 ps, f_{rep} = 1 GHz.	[64]
2013	6 μm × 4 mm multisection RWG, 10 chirpedInAs QD layers. λ tuned by variation in reverse bias.	1245 nm/ 4.8 nm	45 nm (1245–1290 nm)	27 mW average power	Passive ML, shortest Δτ = **3.3 ps,** **f_{rep} = 10 GHz** achieved within λ tuning range	[36]
2013	3.4 μm × 3.9 mm RWG, 7 nonidentical InAs QD layers. λ tuning by band−pass filter	1255 nm	100 nm (1200–1300 nm)		Active ML, Δτ ~ 14−20ps, f_{rep} = 1GHz.	[65]
2013	Gain device comprised 10 layers InAs QDs in EC, λ tuning by prism rotation	1183.5 nm	35.7 nm (1147.8–1183.5 nm)	16 mW average power	Passive ML via SESAM **f_{rep} = 520 MHz**	[61]

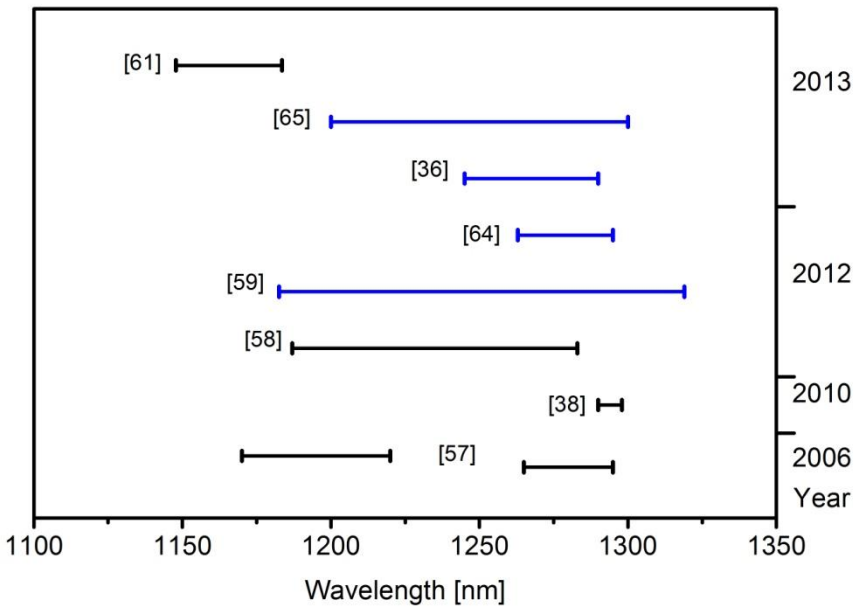

Figure 7. Progress of the tunability ranges along the years, for mode−locked tunable InAs/GaAs QD lasers in the 1–1.3 μm spectral range. QD lasers with chirped layer structures are shown in blue and even layers in black.

Similarly to CW−emitting broadly−tunable QD lasers, there has been a trend from structures containing identical towards non−identical QD layers in more recent times, as these offer an extended broad gain bandwidth (Figure 7).

6. Applications

This section focuses on tunable QD laser systems that not only represent novel developments in particular areas, for example broad wavelength tunability or high power, but have demonstrated significant contribution to real−world applications. The 1–1.3 μm spectral region of light where GaAs−based InAs QD lasers typically operate is particularly useful as it provides deep penetration into biological tissue with low scattering. It is also perfectly placed for frequency doubling into the visible region of light, an area where conventional semiconductor diodes are unable to reach due to a lack of efficient direct bandgap lasers. Systems in place at the moment that target this broad spectral range, for example Ti:Sapphire−pumped optical parametric oscillators, are expensive and bulky to run. QD lasers on the other hand have a smaller footprint, are less complex and less costly and so are suitable replacements especially when tuned to the same range of wavelengths. Very promising results were achieved with multi−photon imaging at fixed wavelength using a mode−locked QD laser system [15], and one could anticipate that the tunability demonstrated before could also be exploited into a more flexible multi−photon configuration [58], where the wavelength could be tuned to target the chromophores of interest. The first demonstration of second−harmonic generation with a broadly tunable QD laser has enabled the access to the yellow spectral region via coupling into an enhancement cavity containing a periodically−poled $LiNbO_3$ (bulk) crystal [44]. In this case, 155 nm of tunability of the fundamental around 1202.5 nm was achieved and a high−finesse cavity was used to reduce the linewidth at 1156 nm down to 30 kHz. Frequency doubling was achieved at 578 nm with ~2.5% efficiency (tunability of the second−harmonic generation was not reported in the paper). This second−harmonic generated radiation was deemed suitable for an Yb optical atomic clock, where the narrow clock transition lies at 578 nm, with the added benefits of reduction in size and cost through use of a laser diode. A higher efficiency of 10.5% was later demonstrated by using a waveguided periodically−poled KTP crystal, end−pumped by a tunable QD laser (150 nm tunability around 1213 nm) [13], resulting in frequency doubling into the orange spectral range (612.9 nm), with a temperature−controlled tunability of 3.4 nm [13]. The use of a waveguided periodically−poled $LiNbO_3$ crystal was also used to significantly boost the efficiency of 578 nm yellow light generation with a QD tunable laser without an enhancement cavity, resulting in yellow light with an output power slightly over 10 mW and a conversion efficiency of around 30% [70].

Very recently, widely tunable second harmonic generation into the visible was demonstrated, covering the spectral region from 574 nm to 647 nm [71]. This 73 nm tunability (not continuous) was achieved by exploiting both the broadband tunability of the fundamental radiation allowed by a multimode QD laser, along with the quasi−phase matching in a multimode waveguided periodically−poled KTP and tapping into the significant difference in the effective refractive indices of the higher and lower−order modes [71], as previously demonstrated in [72]. A maximum power of 12 mW was achieved at 605.6 nm, with an efficiency of 10.3%. This type of technique has also been used to generate picosecond pulses into the orange−to−red spectral region (600–627 nm), using a

tunable QD mode−locked external−cavity laser [73], with maximum efficiency of 4.5%. The access to the visible spectral region, particularly in the yellow range, would be useful for a range of biomedical applications, most notably in ophthalmology [74].

Given the imaging qualities of the 1–1.3 μm spectral region, lasers with these wavelengths are of high relevance in biological imaging, in particular optical coherence tomography (OCT), which uses low−coherence interferometry to capture 3D images from the sub−surface of typically optical scattering biological tissues [75]. A QD SOA swept−source laser was presented in [14], with a full sweep range of 120 nm centered around 1220 nm. The laser (in both grating−coupled Littrow and Littman configurations) was successfully implemented in an OCT setup and in vivo images of palmar skin were taken. The Littrow configuration proved more suitable for this setup, as there was a shorter coherence length (and therefore improved depth resolution) than with the Littman configuration.

Another application is that of THz radiation generation, which has in turn found potential widespread use in security, medical imaging and spectroscopy [46]. A common approach involves photomixing the output of multi−wavelength ECLs [76], and in this respect, tunable QD lasers can offer some advantages by affording broader spectral flexibility and allowing for wider spectral separation of the multiple wavelengths. One such system utilized a double−Littman configuration ECL [46], achieving a maximum wavelength separation of 126 nm for dual lasing, which represents over 25 THz in frequency difference. QD−based lasers have particularly proved their worth in dual−wavelength sources, as due to their broad gain bandwidth, the lasers can remain locked in the dual−wavelength emission regime at a wide range of bias currents and increased temperatures [77], which would be of interest for the uncooled operation of such devices, further reducing complexity, cost and electrical power consumption.

Since the inception of QD lasers, optical communications has been considered one of the primary target applications, as these lasers can easily access the spectral region corresponding to the O−band (1260–1360 nm), replacing lasers based on InP substrates, which are typically more prone to problems due to high non−radiative recombination in InP. More recently, Yamamoto and co−workers have made efforts towards the use of a new optical communications band—the so−called Thousand−band or T−Band, spanning from 1000 nm to 1260 nm, with the aim of expanding capacity for metro/access network systems, optical interconnects and short−haul communications [34]. Both of these bands are easily accessible to QD lasers, and the development of suitable sources for photonic transmission has been one of the major drivers in this field. In this context, recent developments have included a robust QD ECL tuned using multiple band−pass and etalon filters with a wavelength range of 1265–1321 nm, which achieved error−free photonic transmission of a 10 Gb/s signal over 11.4 km of fiber [34]. With only a 0.5 dB loss in power (presumably due to fiber losses), this was evidence of a tunable QD laser being successfully applied to high−speed optical communications. The promise of this work for integration with silicon has been recently materialized with the demonstration of a multi−wavelength external cavity based on a reflective QD SOA integrated with a silicon chip which incorporated a Sagnac loop mirror and a micro−ring filter for four−wavelength emission. By modulating each of the wavelengths, error−free data transmission at 4×10 Gb/s was successfully demonstrated [78].

Finally, while not directly resulting in a broadly−tunable laser, frequency comb lasers are a direct exploration of the broad gain bandwidth offered by QD materials. One of the key outstanding results is the generation of ultra−broadband laser emission with a 75 nm bandwidth [21], due to the combination

of inhomogeneous broadening of the gain and enhanced spectral hole burning associated with these materials. Owing to the low mode partition noise and relative intensity noise associated with QD lasers [79,80], this has also been successfully exploited by a number of groups across the world in the development of highly stable combs which have proved suitable for dense wavelength division multiplexing [81−85]. Moreover, the temperature resilience offered by QD lasers has also enabled the demonstration of wide eye patterns at 25 Gb/s, at temperatures between 40 °C and 80 °C, using the filtered individual modes of a QD comb laser [86]. It was observed that due to the broadband gain, even with the increase in temperature, the same wavelengths remained locked, which matches results previously reported in the context of dual−wavelength QD ECLs coupled with multiplexed volume Bragg gratings [77].

7. Conclusions and Outlook

From the progress up to date, it becomes clear that broadly−tunable QD lasers have achieved significant milestones in the past years. The flexibility of QD structure engineering, chip design, external cavity layout and diverse approaches to continuous wave and mode−locked operation have resulted in a significant variety of laser systems, where trade−offs take an important role—such as for example, the fact that chirped QD structures offer a broad tunability, at the expense of threshold current and temperature sensitivity. The design of the lasers is ultimately driven and shaped by the target applications, bringing to fruition successful demonstrations in biomedical imaging, second−harmonic generation and optical communications. The spectral flexibility afforded by QD lasers at low pump currents has enabled the demonstration of tunabilities up to 208 nm [8] and 136 nm [59] in CW and mode−locked regimes, respectively, while output power levels up to 0.97 W have been achieved [7], outperforming QD−based VECSELs in tunability, power and wallplug efficiency in the same spectral region [50]. It is anticipated that optical power scaling efforts can successfully continue in the near future, supported by QD lasers' enhanced resilience to beam filamentation compared to QW lasers [87,88], and higher threshold of catastrophic optical damage, which is likely to be assisted by a much lower diffusion of carriers towards the laser facets [89].

In terms of tunability, new developments in the integration of QW with QD materials show promise to extend the spectral flexibility even further. A promising approach has shown that by including a QW spectrally aligned with the second excited state of the QD layers, the loss associated with the second excited state can be offset and a 100 nm bandwidth enhancement is achieved, compared to other equivalent QD−only structures, resulting in a modal gain of 300 nm [90]. A laser based on this structure has already demonstrated three−state lasing, at threshold current density 20 times lower than with QD−only lasers [91]. While these results were achieved with identical QD layers, a recent new formulation of the structure including non−identical QD layers has led to the demonstration of a 350 nm wide spontaneous emission spectra [92]. The advance of techniques based on selective area intermixing of QD structures has also resulted in 310 nm bandwidth centered at 1145 nm for a device with three sections with different intermixing properties [93], offering more degrees of freedom on QD structure engineering.

On the other hand, the successful growth of 1.3 μm InAs/GaAs lasers on silicon substrates [94] has built on the fact that QDs are better for this type of integration due to their immunity to threading

dislocations. Following this work, a superluminescent light emitting diode monolithically grown on Si was demonstrated, with a spectrum 114 nm wide and centered at 1255 nm with identical QD layers, where the conditions were optimized to maximize size inhomogeneity [95]. A similar approach was then taken on a germanium substrate, with a 60 nm spectral bandwidth centered at 1252 nm, a bandwidth which showed to be resilient up to an operating temperature of 100 °C [96]. It is highly likely that such materials, initially targeted at superluminescent diodes, will find their way to broadly tunable lasers and ultrafast lasers soon and it is expected that this cross−fertilization will continue in the future.

While this review focused on the InAs/GaAs QD lasers emitting between 1–1.3 μm, the ongoing development of materials in other spectral regions bodes well to the future expansion to other wavelength ranges, most notably in the red [9,97,98] and near−infrared [99] spectral regions, as well as deeper into the infrared (1.7 μm), with a fully integrated tunable QD laser demonstrated recently (1685 nm–1745 nm) [100]. We therefore anticipate that the future will bring many fertile developments in this exciting area of research.

Acknowledgments

S.E. White acknowledges the support from an EPSRC/Wellcome Trust PhD DTA studentship. M.A. Cataluna acknowledges support through a Royal Academy of Engineering/EPSRC Research Fellowship and the Phillip Leverhulme Prize (Leverhulme Trust, PLP−2011−172).

Conflict of Interest

The authors declare no conflict of interest.

References

1. Dingle, R.; Henry, C.H. *Quantum effects in heterostructure lasers*; US Patent No. 3982207; 1976.
2. Arakawa, Y.; Sakaki, H. Multidimensional quantum well laser and temperature dependence of its threshold current. *Appl. Phys. Lett.* **1982**, *40*, 939−941.
3. Goldstein, L.; Glas, F.; Marzin, J.; Charasse, M.; Le Roux, G. Growth by molecular beam epitaxy and characterization of InAs/GaAs strained-layer superlattices. *Appl. Phys. Lett.* **1985**, *47*, 1099−1101.
4. Ledentsov, N.; Ustinov, V.; Egorov, A.Y.; Zhukov, A.; Maksimov, M.; Tabatadze, I.; Kop'ev, P. Optical properties of heterostructures with InGaAs−GaAs quantum clusters. *Semiconductors* **1994**, *28*, 832−834.
5. Kirstaedter, N.; Ledentsov, N.N.; Grundmann, M.; Bimberg, D.; Ustinov, V.M.; Ruvimov, S.S.; Maximov, M.V.; Kop'ev, P.S.; Alferov, Z.I.; Richter, U.; *et al.* Low threshold, large T_o injection laser emission from (InGa)As quantum dots. *Electron. Lett.* **1994**, *30*, 1416−1417.
6. Lv, X.Q.; Jin, P.; Wang, W.Y.; Wang, Z.G. Broadband external cavity tunable quantum dot lasers with low injection current density. *Opt. Express* **2010**, *18*, 8916−8922.

7. Haggett, S.; Krakowski, M.; Montrosset, I.; Cataluna, M.A. High−power quantum−dot tapered tunable external−cavity lasers based on chirped and unchirped structures. *Opt. Express* **2014**, *22*, 22854−22864.
8. Lv, X.; Jin, P.; Wang, Z. Broadly tunable grating−coupled external cavity laser with quantum−dot active region. *IEEE Photon. Technol. Lett.* **2010**, *22*, 1799−1801.
9. Schulz, W.M.; Eichfelder, M.; Roßbach, R.; Jetter, M.; Michler, P. InP/AlGaInP quantum dot laser emitting at 638 nm. *J. Cryst. Growth* **2011**, *315*, 123−126.
10. Ustinov, V.M.; Zhukov, A.E.; Egorov, A.Y.; Kovsh, A.R.; Zaitsev, S.V.; Gordeev, N.Y.; Kopchatov, V.I.; Ledentsov, N.N.; Tsatsul'nikov, A.F.; Volovik, B.V.; *et al.* Low threshold quantum dot injection laser emitting at 1.9 μm. *Electron. Lett.* **1998**, *34*, 670−672.
11. Ustinov, V.M.; Zhukov, A.E.; Egorov, A.Y.; Maleev, N.A. *Quantum dot lasers*; Oxford University Press: New York, NY, USA, 2003.
12. Orr, B.J.; He, Y. Rapidly swept continuous−wave cavity−ringdown spectroscopy. *Chem. Phys. Lett.* **2011**, *512*, 1−20.
13. Fedorova, K.; Cataluna, M.; Battle, P.; Kaleva, C.; Krestnikov, I.; Livshits, D.; Rafailov, E. Orange light generation from a PPKTP waveguide end pumped by a CW quantum−dot tunable laser diode. *Appl. Phys. B* **2011**, *103*, 41−43.
14. Krstajic, N.; Childs, D.T.; Matcher, S.; Livshits, D.; Shkolnik, A.; Krestnikov, I.; Hogg, R. Swept−source laser based on quantum−dot semiconductor optical amplifier—applications in optical coherence tomography. *IEEE Photon. Technol. Lett.* **2011**, *23*, 739−741.
15. Ding, Y.; Aviles−Espinosa, R.; Cataluna, M.; Nikitichev, D.; Ruiz, M.; Tran, M.; Robert, Y.; Kapsalis, A.; Simos, H.; Mesaritakis, C.; *et al.* High peak−power picosecond pulse generation at 1.26 μm using a quantum−dot−based external−cavity mode−locked laser and tapered optical amplifier. *Opt. Express* **2012**, *20*, 14308−14320.
16. Kobat, D.; Durst, M.E.; Nishimura, N.; Wong, A.W.; Schaffer, C.B.; Xu, C. Deep tissue multiphoton microscopy using longer wavelength excitation. *Opt. Express* **2009**, *17*, 13354−13364.
17. Ledentsov, N.N.; Grundmann, M.; Heinrichsdorff, F.; Bimberg, D.; Ustinov, V.; Zhukov, A.; Maximov, M.; Alferov, Z.I.; Lott, J. Quantum−dot heterostructure lasers. *IEEE J. Sel. Top. Quantum Electron.* **2000**, *6*, 439−451.
18. Zhukov, A.; Kovsh, A.; Ustinov, V. Temperature dependence of the gain of lasers based on quantum−dot arrays with an inhomogeneously broadened density of states. *Semiconductors* **1999**, *33*, 1260−1264.
19. Qasaimeh, O. Effect of inhomogeneous line broadening on gain and differential gain of quantum dot lasers. *IEEE Trans. Electron Devices* **2003**, *50*, 1575–1581.
20. Rafailov, E.U.; Cataluna, M.A.; Sibbett, W. Mode−locked quantum−dot lasers. *Nat. Photon.* **2007**, *1*, 395−401.
21. Kovsh, A.; Krestnikov, I.; Livshits, D.; Mikhrin, S.; Weimert, J.; Zhukov, A. Quantum dot laser with 75 nm broad spectrum of emission. *Opt. Lett.* **2007**, *32*, 793−795.
22. Fedorova, K.A.; Cataluna, M.A.; Krestnikov, I.; Livshits, D.; Rafailov, E.U. Broadly tunable high−power InAs/GaAs quantum−dot external cavity diode lasers. *Opt. Express* **2010**, *18*, 19438−19443.

23. Sun, Z.Z.; Ding, D.; Gong, Q.; Zhou, W.; Xu, B.; Wang, Z.G. Quantum−dot superluminescent diode: A proposal for an ultra−wide output spectrum. *Opt. Quantum Electron.* **1999**, *31*, 1235−1246.
24. Heo, D.C.; Song, J.D.; Choi, W.J.; Lee, J.I.; Jung, J.C.; Han, I.K. High power broadband InGaAs/GaAs quantum dot superluminescent diodes. *Electron. Lett.* **2003**, *39*, 863−865.
25. Zhang, Z.Y.; Wang, Z.G.; Xu, B.; Jin, P.; Sun, Z.Z.; Liu, F.Q. High−performance quantum−dot superluminescent diodes. *IEEE Photon. Technol. Lett.* **2004**, *16*, 27−29.
26. Li, L.; Rossetti, M.; Fiore, A.; Occhi, L.; Vélez, C. Wide emission spectrum from superluminescent diodes with chirped quantum dot multilayers. *Electron. Lett.* **2005**, *41*, 41−43.
27. Ray, S.K.; Groom, K.M.; Beattie, M.D.; Liu, H.Y.; Hopkinson, M.; Hogg, R.A. Broad−band superluminescent light−emitting diodes incorporating quantum dots in compositionally modulated quantum wells. *IEEE Photon. Technol. Lett.* **2006**, *18*, 58−60.
28. Rossetti, M.; Li, L.; Markus, A.; Fiore, A.; Occhi, L.; Vélez, C.; Mikhrin, S.; Krestnikov, I.; Kovsh, A. Characterization and modeling of broad spectrum InAs−GaAs quantum−dot superluminescent diodes emitting at 1.2−1.3 μm. *IEEE J. Quantum Electron.* **2007**, *43*, 676−686.
29. Chen, J.X.; Markus, A.; Fiore, A.; Oesterle, U.; Stanley, R.P.; Carlin, J.F.; Houdré, R.; Ilegems, M.; Lazzarini, L.; Nasi, L.; *et al.* Tuning InAs/GaAs quantum dot properties under Stranski−Krastanov growth mode for 1.3 μm applications. *J. Appl. Phys.* **2002**, *91*, 6710−6716.
30. Nishi, K.; Saito, H.; Sugou, S.; Lee, J.-S. A narrow photoluminescence linewidth of 21 meV at 1.35 μm from strain−reduced InAs quantum dots covered by $In_{0.2}Ga_{0.8}As$ grown on GaAs substrates. *Appl. Phys. Lett.* **1999**, *74*, 1111−1113.
31. Volovik, B.; Tsatsul'nikov, A.; Bedarev, D.; Egorov, A.Y.; Zhukov, A.; Kovsh, A.; Ledentsov, N.; Maksimov, M.; Maleev, N.; Musikhin, Y.G. Long−wavelength emission in structures with quantum dots formed in the stimulated decomposition of a solid solution at strained islands. *Semiconductors* **1999**, *33*, 901−905.
32. Ye, C.; Wei, T.K. *Tunable external cavity diode lasers*; World Scientific: Hackensack, NJ, USA, 2004.
33. Tierno, A.; Ackemann, T. Tunable, narrow−band light source in the 1.25 μm region based on broad−area quantum dot lasers with feedback. *Appl. Phys. B* **2007**, *89*, 585−588.
34. Yamamoto, N.; Akahane, K.; Kawanishi, T.; Omigawa, Y.; Sotobayashi, H.; Yoshioka, Y.; Takai, H. Narrow−line−width 1.31−μm wavelength tunable quantum dot laser using sandwiched sub−nano separator growth technique. *Opt. Express* **2011**, *19*, B636−B644.
35. Kaiser, W.; Deubert, S.; Reithmaier, J.; Forchel, A. Singlemode tapered quantum dot laser diodes with monolithically integrated feedback gratings. *Electron. Lett.* **2007**, *43*, 926−927.
36. Nikitichev, D.I.; Cataluna, M.A.; Fedorova, K.A.; Ding, Y.; Mikhrin, S.S.; Krestnikov, I.L.; Livshits, D.A.; Rafailov, E.U. High−power wavelength bistability and tunability in passively mode−locked quantum−dot laser. *IEEE J. Sel. Top. Quant. Electron.* **2013**, *19*, 1100907.
37. Stevens, B.; Childs, D.; Groom, K.; Hopkinson, M.; Hogg, R. All semiconductor swept laser source utilizing quantum dots. *Appl. Phys. Lett.* **2007**, *91*, 121119.
38. Habruseva, T.; O'Donoghue, S.; Rebrova, N.; Reid, D.A.; Barry, L.P.; Rachinskii, D.; Huyet, G.; Hegarty, S.P. Quantum−dot mode−locked lasers with dual mode optical injection. *IEEE Photon. Technol. Lett.* **2010**, *22*, 359−361.

39. Eliseev, P.; Li, H.; Stintz, A.; Liu, G.; Newell, T.; Malloy, K.; Lester, L. Tunable grating−coupled laser oscillation and spectral hole burning in an InAs quantum−dot laser diode. *IEEE J. Quantum Electron.* **2000**, *36*, 479−485.
40. Li, H.; Liu, G.; Varangis, P.; Newell, T.; Stintz, A.; Fuchs, B.; Malloy, K.; Lester, L. 150−nm tuning range in a grating−coupled external cavity quantum−dot laser. *IEEE Photon. Technol. Lett.* **2000**, *12*, 759−761.
41. Varangis, P.M.; Li, H.; Liu, G.T.; Newell, T.C.; Stintz, A.; Fuchs, B.; Malloy, K.J.; Lester, L.F. Low−threshold quantum dot lasers with 201 nm tuning range. *Electron. Lett.* **2000**, *36*, 1544−1545.
42. Biebersdorf, A.; Lingk, C.; De Giorgi, M.; Feldmann, J.; Sacher, J.; Arzberger, M.; Ulbrich, C.; Böhm, G.; Amann, M.; Abstreiter, G. Tunable single and dual mode operation of an external cavity quantum−dot injection laser. *J. Phys. D: Appl. Phys.* **2003**, *36*, 1928.
43. Stevens, B.J.; Childs, D.T.D.; Groom, K.M.; Hopkinson, M.; Hogg, R.A. A quantum dot swept laser source based upon a multisection laser device. *Jpn. J. Appl. Phys.* **2008**, *47*, 2965−2967.
44. Nevsky, A.Y.; Bressel, U.; Ernsting, I.; Eisele, C.; Okhapkin, M.; Schiller, S.; Gubenko, A.; Livshits, D.; Mikhrin, S.; Krestnikov, I. A narrow−line−width external cavity quantum dot laser for high−resolution spectroscopy in the near−infrared and yellow spectral ranges. *Appl. Phys. B* **2008**, *92*, 501−507.
45. Lin, G.; Su, P.-Y.; Cheng, H.-C. Low threshold current and widely tunable external cavity lasers with chirped multilayer InAs/InGaAs/GaAs quantum−dot structure. *Opt. Express* **2012**, *20*, 3941−3947.
46. Pai, C.-H.; Lin, G. Tunable multiwavelength quantum dot external−cavity lasers. *Proc. SPIE* **2013**, *8772*, 87720V−87727.
47. Seltzer, C.; Bagley, M.; Elton, D.; Perrin, S.; Cooper, D. 160 nm continuous tuning of an MQW laser in an external cavity across the entire 1.3 μm communications window. *Electron. Lett.* **1991**, *27*, 95−96.
48. Anscombe, N. Tapered triumph. *Nature Photon.* **2009**, *3*, 24−25.
49. Albrecht, A.R.; Stintz, A.; Jaeckel, F.T.; Rotter, T.J.; Ahirwar, P.; Patel, V.J.; Hains, C.P.; Lester, L.F.; Malloy, K.J.; Balakrishnan, G. 1220–1280−nm Optically Pumped InAs Quantum Dot−Based Vertical External−Cavity Surface−Emitting Laser. *IEEE J. Sel. Top. Quantum Electron.* **2011**, *17*, 1787−1793.
50. Butkus, M.; Rautiainen, J.; Okhotnikov, O.G.; Hamilton, C.J.; Malcolm, G.; Mikhrin, S.; Krestnikov, I.L.; Livshits, D.; Rafailov, E.U. Quantum dot based semiconductor disk lasers for 1–1.3 μm. *IEEE J. Sel. Top. Quantum Electron.* **2011**, *17*, 1763−1771.
51. Rafailov, E.U.; Cataluna, M.A.; Avrutin, E.A. *Ultrafast Lasers Based on Quantum Dot Structures: Physics and Devices*; Wiley: Weinheim, Germany, 2011.
52. Cataluna, M.A.; Ding, Y.; Nikitichev, D.I.; Fedorova, K.A.; Rafailov, E.U. High−power versatile picosecond pulse generation from mode−locked quantum−dot laser diodes. *IEEE J. Sel. Top. Quantum Electron.* **2011**, *17*, 1302−1310.
53. Schneider, S.; Borri, P.; Langbein, W.; Woggon, U.; Sellin, R.L.; Ouyang, D.; Bimberg, D. Excited−state gain dynamics in InGaAs quantum−dot amplifiers. *IEEE Photon. Technol. Lett.* **2005**, *17*, 2014−2016.

54. Piwonski, T.; Pulka, J.; Madden, G.; Huyet, G.; Houlihan, J.; Viktorov, E.A.; Erneux, T.; Mandel, P. Intradot dynamics of InAs quantum dot based electroabsorbers. *Appl. Phys. Lett.* **2009**, *94*, 123504.
55. Cataluna, M.A.; Sibbett, W.; Livshits, D.A.; Weimert, J.; Kovsh, A.R.; Rafailov, E.U. Stable mode locking via ground−or excited−state transitions in a two−section quantum−dot laser. *Appl. Phys. Lett.* **2006**, *89*, 081124.
56. Cataluna, M.A.; Rafailov, E.U.; McRobbie, A.D.; Sibbett, W.; Livshits, D.A.; Kovsh, A.R. Ground and excited−state modelocking in a two−section quantum−dot laser. In Proceedings of the Lasers and Electro−Optics Society Annual Meeting−LEOS, Lasers and Electro−Optics Society Annual Meeting−LEOS, Sydney, Australia, 22−28 October 2005; pp. 870−871.
57. Kim, J.; Choi, M.-T.; Lee, W.; Delfyett, P.J.; Jr. Wavelength tunable mode−locked quantum−dot laser. *Proc. SPIE* **2006**, *6243*, 62430M−62438.
58. Ding, Y.; Alhazime, A.; Nikitichev, D.; Fedorova, K.; Ruiz, M.; Tran, M.; Robert, Y.; Kapsalis, A.; Simos, H.; Mesaritakis, C.; *et al.* Tunable master−oscillator power−amplifier based on chirped quantum−dot structures. *IEEE Photon. Technol. Lett.* **2012**, *24*, 1841−1844.
59. Nikitichev, D.; Fedorova, K.; Ding, Y.; Alhazime, A.; Able, A.; Kaenders, W.; Krestnikov, I.; Livshits, D.; Rafailov, E. Broad wavelength tunability from external cavity quantum−dot mode−locked laser. *Appl. Phys. Lett.* **2012**, *101*, 121107.
60. McRobbie, A.D.; Cataluna, M.A.; Zolotovskaya, S.A.; Livshits, D.A.; Sibbett, W.; Rafailov, E.U. High power all−quantum−dot−based external cavity modelocked laser. *Electron. Lett.* **2007**, *43*, 812−813.
61. Wu, J.; Jin, P.; Li, X.-K.; Wei, H.; Wu, J.; Wang, Z.-G. Tunable mode−locked external−cavity quantum−dot laser. In Proceedings of the International Photonics and Optoelectronics Meetings (POEM), Wuhan; China, 25−26 May 2013; p. NSu2B. 3.
62. Cheng, H.C.; Wu, Q.Y.; Pan, C.H.; Lee, C.P.; Lin, G. Low repetition rate and broad frequency tuning from a grating−coupled passively mode−locked quantum dot laser. *Appl. Phys. Lett.* **2013**, *103*, 211109.
63. Ding, Y.; Cataluna, M.A.; Nikitichev, D.; Krestnikov, I.; Livshits, D.; Rafailov, E. Broad repetition−rate tunable quantum−dot external−cavity passively mode−locked laser with extremely narrow radio frequency linewidth. *Appl. Phys. Express* **2011**, *4*, 062703.
64. Yamamoto, N.; Akahane, K.; Tetsuya, K.; Sotobayashi, H.; Yoshioka, Y.; Takai, H. Characterization of wavelength−tunable quantum dot external cavity laser for 1.3−μm−waveband coherent light sources. *Jpn. J. Appl. Phys.* **2012**, *51*, 02BG08.
65. Yamamoto, N.; Akahane, K.; Kawanishi, T.; Sotobayashi, H.; Yoshioka, Y.; Takai, H. 10−GHz high−repetition optical short pulse generation from wavelength−tunable quantum dot optical frequency comb laser. *IEICE Trans. Electron.* **2013**, doi:10.1587/transele.E96.C.187.
66. Derickson, D.J.; Helkey, R.J.; Mar, A.; Karin, J.R.; Wasserbauer, J.G.; Bowers, J.E. Short pulse generation using multisegment mode−locked semiconductor lasers. *IEEE J. Quantum Electron.* **1992**, *28*, 2186−2202.
67. Derickson, D.J.; Morton, P.A.; Bowers, J.E.; Thornton, R.L. Comparison of timing jitter in external and monolithic cavity mode−locked semiconductor lasers. *Appl. Phys. Lett.* **1991**, *59*, 3372−3374.

68. Mesaritakis, C.; Simos, C.; Simos, H.; Krestnikov, I.; Syvridis, D. Dual ground−state pulse generation from a passively mode−locked InAs/InGaAs quantum dot laser. *Appl. Phys. Lett.* **2011**, *99*, 141109.
69. Cataluna, M.A.; Nikitichev, D.I.; Mikroulis, S.; Simos, H.; Simos, C.; Mesaritakis, C.; Syvridis, D.; Krestnikov, I.; Livshits, D.; Rafailov, E.U. Dual−wavelength mode−locked quantum−dot laser, via ground and excited state transitions: Experimental and theoretical investigation. *Opt. Express* **2010**, *18*, 12832−12838.
70. Lee, W.-K.; Park, C.Y.; Yu, D.-H.; Park, S.E.; Lee, S.-B.; Kwon, T.Y. Generation of 578−nm yellow light over 10 mW by second harmonic generation of an 1156−nm external−cavity diode laser. *Opt. Express* **2011**, *19*, 17453−17461.
71. Fedorova, K.; Sokolovskii, G.; Battle, P.; Livshits, D.; Rafailov, E. 574–647 nm wavelength tuning by second−harmonic generation from diode−pumped PPKTP waveguides. *Opt. Lett.* **2015**, *40*, 835−838.
72. Fedorova, K.A.; Sokolovskii, G.S.; Battle, P.R.; Livshits, D.A.; Rafailov, E.U. Green−to−red tunable SHG of a quantum−dot laser in a PPKTP waveguide. *Las. Phys. Lett.* **2012**, *9*, 790−795.
73. Fedorova, K.; Sokolovskii, G.; Nikitichev, D.; Battle, P.; Krestnikov, I.; Livshits, D.; Rafailov, E. Orange−to−red tunable picosecond pulses by frequency doubling in a diode−pumped PPKTP waveguide. *Opt. Lett.* **2013**, *38*, 2835−2837.
74. Jensen, O.B.; Hansen, A.K.; Muller, A.; Sumpf, B.; Unterhuber, A.; Drexler, W.; Petersen, P.M.; Andersen, P.E. Power scaling of nonlinear frequency converted tapered diode lasers for biophotonics. *IEEE J. Sel. Top. Quantum Electron.* **2014**, *20*, 307−321.
75. Schmitt, J.M. Optical coherence tomography (OCT): A review. *IEEE J. Sel. Top. Quantum Electron.* **1999**, *5*, 1205−1215.
76. Hoffmann, S.; Hofmann, M.R. Generation of Terahertz radiation with two color semiconductor lasers. *Las. Photon. Rev.* **2007**, *1*, 44−56.
77. Daghestani, N.; Cataluna, M.; Ross, G.; Rose, M. Compact dual−wavelength InAs/GaAs quantum−dot external−cavity laser stabilized by a single volume Bragg grating. *IEEE Photon. Technol. Lett.* **2011**, *23*, 176−178.
78. Zhang, Y.; Yang, S.; Zhu, X.; Li, Q.; Guan, H.; Magill, P.; Bergman, K.; Baehr−Jones, T.; Hochberg, M. Quantum dot SOA/silicon external cavity multi−wavelength laser. *Opt. Express* **2015**, *23*, 4666−4671.
79. Krakowski, M.; Resneau, P.; Calligaro, M.; Liu, H.; Hopkinson, M. High Power, Very Low Noise, CW Operation of 1.32μm Quantum−Dot Fabry−Perot Laser Diodes. In Proceedings of the IEEE 20th International Semiconductor Laser Conference, Kohala Coast, HI, USA, 17−21 September 2006; pp. 39−40.
80. Capua, A.; Rozenfeld, L.; Mikhelashvili, V.; Eisenstein, G.; Kuntz, M.; Laemmlin, M.; Bimberg, D. Direct correlation between a highly damped modulation response and ultra low relative intensity noise in an InAs/GaAs quantum dot laser. *Opt. Express* **2007**, *15*, 5388−5393.
81. Gubenko, A.; Krestnikov, I.; Livshtis, D.; Mikhrin, S.; Kovsh, A.; West, L.; Bornholdt, C.; Grote, N.; Zhukov, A. Error−free 10 Gbit/s transmission using individual Fabry−Perot modes of low−noise quantum−dot laser. *Electron. Lett.* **2007**, *43*, 1430−1431.

82. Kovsh, A.; Gubenko, A.; Krestnikov, I.; Livshits, D.; Mikhrin, S.; Weimert, J.; West, L.; Wojcik, G.; Yin, D.; Bornholdt, C.; *et al.* Quantum dot comb−laser as efficient light source for silicon photonics. *Proc. SPIE* **2008**, *6996*, 69960V.
83. Livshits, D.; Yin, D.; Gubenko, A.; Krestnikov, I.; Mikhrin, S.; Kovsh, A.; Wojcik, G. Cost−effective WDM optical interconnects enabled by quantum dot comb lasers. *Proc. SPIE* **2010**, *7607*, 76070W.
84. Lee, C.S.; Guo, W.; Basu, D.; Bhattacharya, P. High performance tunnel injection quantum dot comb laser. *Appl. Phys. Lett.* **2010**, *96*, 101107.
85. Yausoka, N.; Ishida, M.; Takada, K.; Yamaguchi, M.; Yamamoto, T.; Arakawa, Y. Low−noise four−wavelength simultaneous oscillation of a 1.3−μm external−cavity quantum−dot laser. *Proc. SPIE* **2015**, *9373*, 937304.
86. Yasuoka, N.; Ishida, M.; Yamaguchi, M.; Uetake, A.; Yamamoto, T.; Arakawa, Y. 1.3 μm External−Cavity Quantum−Dot Comb Laser for Temperature Control Free Operation. In Proceedings of the Optical Fiber Communication Conference, Los Angeles, CA, USA, 22−26 March 2015; p. Tu3I.3.
87. Smowton, P.M.; Pearce, E.J.; Schneider, H.C.; Chow, W.W.; Hopkinson, M. Filamentation and linewidth enhancement factor in InGaAs quantum dot lasers. *Appl. Phys. Lett.* **2002**, *81*, 3251−3253.
88. Ribbat, C.; Sellin, R.L.; Kaiander, I.; Hopfer, F.; Ledentsov, N.N.; Bimberg, D.; Kovsh, A.R.; Ustinov, V.M.; Zhukov, A.E.; Maximov, M.V. Complete suppression of filamentation and superior beam quality in quantum−dot lasers. *Appl. Phys. Lett.* **2003**, *82*, 952−954.
89. Moore, S.A.; O'Faolain, L.; Cataluna, M.A.; Flynn, M.B.; Kotlyar, M.V.; Krauss, T.F. Reduced surface sidewall recombination and diffusion in quantum−dot lasers. *IEEE Photon. Technol. Lett.* **2006**, *18*, 1861−1863.
90. Chen, S.; Zhou, K.; Zhang, Z.; Childs, D.; Hugues, M.; Ramsay, A.; Hogg, R. Ultra−broad spontaneous emission and modal gain spectrum from a hybrid quantum well/quantum dot laser structure. *Appl. Phys. Lett.* **2012**, *100*, 041118.
91. Chen, S.; Zhou, K.; Zhang, Z.; Wada, O.; Childs, D.; Hugues, M.; Jin, X.; Hogg, R. Room temperature simultaneous three−state lasing in hybrid quantum well/quantum dot laser. *Electron. Lett.* **2012**, *48*, 644−645.
92. Peyvast, N.; Chen, S.; Zhou, K.; Babazadeh, N.; Khozim, A.; Zhang, Z.; Childs, D.; Wada, O.; Hugues, M.; Hogg, R. Development of broad spectral bandwidth hybrid QW/QD structures from 1000−1400 nm. *Proc. SPIE* **2014**, *9002*, 900204.
93. Zhou, K.; Jiang, Q.; Zhang, Z.; Chen, S.; Liu, H.; Lu, Z.; Kennedy, K.; Matcher, S.; Hogg, R. Quantum dot selective area intermixing for broadband light sources. *Opt. Express* **2012**, *20*, 26950−26957.
94. Wang, T.; Liu, H.; Lee, A.; Pozzi, F.; Seeds, A. 1.3−μm InAs/GaAs quantum−dot lasers monolithically grown on Si substrates. *Opt. Express* **2011**, *19*, 11381−11386.
95. Chen, S.; Tang, M.; Jiang, Q.; Wu, J.; Dorogan, V.G.; Benamara, M.; Mazur, Y.I.; Salamo, G.J.; Smowton, P.; Seeds, A. InAs/GaAs quantum−dot superluminescent light−emitting diode monolithically grown on a Si substrate. *ACS Photon.* **2014**, *1*, 638−642.

96. Jiang, Q.; Tang, M.; Chen, S.; Wu, J.; Seeds, A.; Liu, H. InAs/GaAs quantum−dot superluminescent diodes monolithically grown on a Ge substrate. *Opt. Express* **2014**, *22*, 23242−23248.
97. Fafard, S.; Hinzer, K.; Raymond, S.; Dion, M.; McCaffrey, J.; Feng, Y.; Charbonneau, S. Red−emitting semiconductor quantum dot lasers. *Science* **1996**, *274*, 1350−1353.
98. Smowton, P.M.; Lutti, J.; Lewis, G.M.; Krysa, A.B.; Roberts, J.S.; Houston, P.A. InP−GaInP quantum−dot lasers emitting between 690−750 nm. *IEEE J. Sel. Top. Quantum Electron.* **2005**, *11*, 1035−1040.
99. Schlereth, T.W.; Schneider, C.; Gerhard, S.; Höfling, S.; Forchel, A. Short−wavelength (760−920 nm) AlGaInAs quantum dot lasers. *IEEE J. Sel. Top. Quantum Electron.* **2009**, *15*, 792−798.
100. Tilma, B.W.; Jiao, Y.; Kotani, J.; Smalbrugge, B.; Ambrosius, H.P.M.M.; Thijs, P.J.; Leijtens, X.J.M.; Nötzel, R.; Smit, M.K.; Bente, E.A.J.M. Integrated tunable quantum−dot laser for optical coherence tomography in the 1.7 μm wavelength region. *IEEE J. Quantum Electron.* **2012**, *48*, 87−98.